Modified Maximum Principal Stress Criterion for Propellant Liner Bond Failures

T. L. Kuhlmann,* R. L. Peeters,† and K. W. Bills Jr.‡
Aerojet Strategic Propulsion Company, Sacramento, California

The structural characterization of propellant liner insulation bond systems in solid rocket motors has been improved through the use of a modified maximum principal stress failure criterion. This failure criterion provides a consistent method for reducing laboratory test failure data and extrapolating the results to predict bondline failures at other stress states and environmental conditions. This improved method of engineering analysis evolved in conjunction with the development of a test specimen that can be used to analog the grain-to-case loading conditions. Another engineering approach currently used that also accurately models the experimental test data calculates the magnitudes of the maximum normal and maximum shear stress components along the bondline of the motor. The individual component values are then compared to the stress-at-break values in tensile and shear tests of bondline specimens. Bond test data, using specimens pulled at angles to give simultaneous tensile and shear stress components, show that the method can be improved by applying the appropriate stress concentration factors. These stress concentration factors were determined from finite-element analyses of the bond specimen. Using a similar approach, it was shown that the modified maximum principal stress failure criterion accurately models specimen bondline failures for all pull angles and pressures considered. The testing procedures and methods of analysis used to evaluate these, as well as several other failure criteria, are presented.

Nonmenclature

A	= sample area minus unbonded (flapped) area; bonded area
a_p	= time pressure shift factor
a_T	= time temperature shift factor
F	= maximum load during test
F/A	= force/area = experimental value of the average stress at maximum load
F_1, F_0, and F_{th}	= the forces corresponding to σ_1, σ_0, and σ_{th}, respectively
m	= slope of the log stress vs log-reduced time regression line
P	= superimposed pressure
SR	= stress ratio = ratio of maximum principal stress at the bondline to average bond stress (obtained from stress analysis of the test specimen)
t_m	= time-to-maximum stress
σ_1	= maximum principal stress at maximum load
σ_0	= reference value of σ_1 at unit time (normally taken as $t_m = 1$ min)
σ_{th}	= a threshold stress value of σ_1 (a value below which no failure will occur)

Introduction and Background

THE effort described in this paper came about in conjunction with a program to develop the rectangular analog bond test specimen.[1] This specimen (and similar specimens[2,3]) was developed to allow testing at various pull angles, which is advantageous for accurately modeling the state of stress at the bondline of solid rocket motors. In that program, bond test data were obtained at various pull angles, loading rates, temperatures, and pressures. The examination and evaluation of this data led to the consideration of how a failure criterion would relate this information to the bond stresses in a solid rocket motor.

The rectangular analog bond specimen (Fig. 1) consists of a 1-in.-thick, 2-in.-high, 4-in.-wide block of propellant, liner, and insulation fully bonded at the propellant-to-end-tab side, and partially (60% by area) bonded at the insulation-to-end-tab side. A "release flap" 0.8 in. long is left unbonded at each end of the specimen. The end of the release flap produces a stress singularity that causes the highest bondline stresses to occur at the flap release points at the "midplane" (i.e., halfway through the thickness) of the specimen, away from the corners. The release flaps also decrease failures of the propellant-to-end-tab "secondary bond" by providing a larger amount of bonding area on the "secondary" side.

The purpose of a failure critierion is to predict when a structural body will cease to function, i.e., fail. In solid rocket motors, the key steps in generating failure criteria for the bondline are 1) testing a structural analog of the bondline (i.e., test specimen), 2) measuring the limiting or failure-producing value of stress or strain, and 3) generalizing the results to the motor by assuming that when the limiting value of the stress or strain is exceeded, failure occurs. The assumption that a state of stress which produces failures in bond test specimens will produce similar failures in solid rocket motors seems reasonable; however, test data to substantiate this assumption are not usually available.

The basic concept of this study is to vary the state of stress at the bondline of the test specimen by varying the pull angle and determining which of the failure criteria provide a limiting (i.e., failure-producing) value. The ultimate goal is to provide accurate bondline failure predictions for all states of stress, times-to-failure, temperatures, and superimposed pressures.

Theory

In this program, the failure criteria examined were limited to stress-based criteria. Strain-based criteria were not con-

Presented as Paper 85-1439 at the AIAA/SAE/ASME/ASEE 21st Joint Propulsion Conference, Monterey, CA, July 8-10, 1985; received Aug. 9, 1985; revision received Sept. 18, 1986.

*Engineer, Propellant Characterization and Analyses Department.
†Engineering Manager, Propellant Characterization and Analyses Department. Member AIAA.
‡Associate Scientist, Chemical Research and Development Division.

sidered because bond tests do not have a singular yield point. The strain yield point depends on the configuration of the test specimen used and other factors that are impossible to relate to motor conditions. Fracture energy evaluation methods were not examined because their usefulness is strongly dependent on having additional, highly accurate, mechanical property values for the materials involved. Stress-based criteria are simpler than fracture-energy methods and are directly applicable to the stress analysis techniques used to calculate bondline margins of safety.

There are a number of different stress criteria currently used to predict bondline failures. The most common include the maximum normal and shear stress components, maximum principal, maximum deviatoric, maximum shear, and maximum octahedral shear stress failure criteria. By observation, the criteria that fit the experimental data best were a modified version of the maximum principal stress and the maximum bond normal and maximum bond shear component failure criteria.

Maximum Bondline Normal and Shear Component Failure Criterion

The maximum bond normal (i.e., tension) and maximum bond shear stress criterion considers the liner to act as an adhesive between two planes. One plane is the propellant and the other is the insulation. Failure is assumed to occur when the strength of the joint (either tensile or shear) is exceeded. This failure criterion considers bondline failures to be one-dimensional events, independent of the overall state of stress in the area. Since the application of superimposed pressure causes all bondline normal stresses to go compressive, the maximum bond tensile failure criterion must be replaced by a deviatoric criterion in the pressurized condition.

Modified Maximum Principal Stress Failure Criterion

This failure criterion was developed specifically for bondline failures by Bills[4] in 1964. It is a modified version of the maximum principal stress criterion and resembles a deviatoric criterion. The following development assumes that failure occurs at the time of maximum load on the load vs time trace of a constant-rate bond test (experimental observation verified this assumption). The maximum principal stress is presented in equation form as follows:

$$\sigma_1 = \sigma_{th} + (\sigma_0 - \sigma_{th})(t_m/a_T a_p)^m \quad (1)$$

The principal stress terms are related to the experimental values as follows:

$$\sigma_1 = SR(F_1/A) - P \quad (2)$$

$$\sigma_0 = SR(F_0/A) - P \quad (3)$$

$$\sigma_{th} = SR(F_{th}/A) - P \quad (4)$$

The methods used to obtain each of the terms in Eqs. (1–4) will be discussed later.

The primary stress value associated with the bond failure (which is taken as the basis for comparison with other failure criteria) is the quantity $\sigma_1 - \sigma_{th}$. The other terms in the equation account for changes in material strength resulting from changes in time-to-failure, temperature, and superimposed hydrostatic pressure. The bond failure stress criterion becomes

$$\sigma_1 - \sigma_{th} = (\sigma_0 - \sigma_{th})(t_m/a_T a_p)^m \quad (5)$$

This failure criterion corresponds viscoelastically to stress relaxation, where the rate of change depends upon the current magnitude above a threshold level.

According to Eq. (5), the failure stress differences ignore pressure except for their effect upon the time-to-failure through a_p. Thus, by adjusting a_T and a_p, the maximum principal stress relation can be applied to relate all temperatures and pressures without modification. Equation (5) resembles a deviatoric criterion; however, the two differ significantly when a state of hydrostatic stress is approached. In that case, the deviatoric stress approaches zero, making that failure criterion impossible to use, while Eq. (5) still rigorously applies.

Experimental Evaluation

As discussed in the introduction, the testing done in this program was an extension of the development program for the rectangular analog bond test specimen (Fig. 1). Low-elongation HTPB propellant (88% solids) was used. The testing consisted of at least three rectangular analog specimens per crosshead rate, three crosshead rates per angle, and pull angles that ranged from 0 deg (shear) to 90 deg (tension) in 15-deg increments. All tests were performed at 77°F and the test plan was carried out at pressures of 0 and 1650 psig. Test data is provided in Table 1. Shear testing with pressure was not performed because of safety considerations; it was feared that friction between the release flap and the end tab would ignite the propellant. The average stress-at-break values at $t_m = 1$ min for the nonpressurized condition are plotted as a function of the pull angle in Fig. 2. The average stress-at-break values were obtained by running a regression line through the log stress vs log time-to-maximum stress data for each pull angle. The $t_m = 1$ min values were used for convenience. Since the slopes of all regression lines were approximately equal, any time value could have been used for comparison. The failure criterion investigation program described in this paper was an effort to explain the variation of bond strength as a function of pull angle (i.e., state of stress).

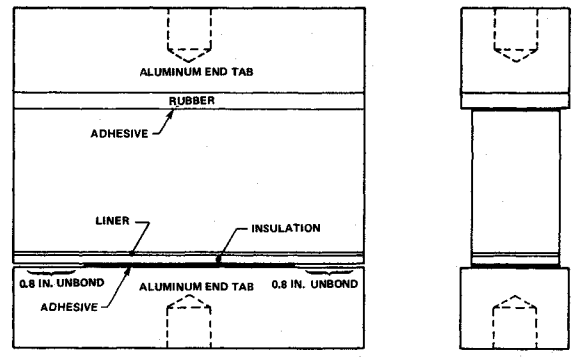

Fig. 1 Rectangular analog bond specimen.

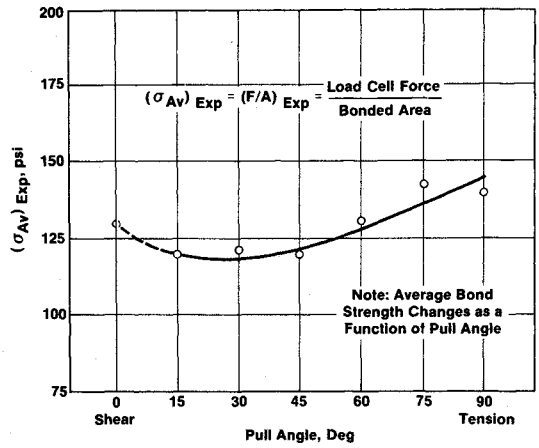

Fig. 2 Average bond strenth vs pull angle.

Stress Analysis

The analyses used to obtain the stress distribution in the specimen at the various pull angles were performed using the TEXGAP two-dimensional, linear elastic, finite-element computer code.[5] The propellant, liner, insulation, adhesive, and aluminum end tabs were modeled in the configuration shown in Fig. 1. A plane stress solution was used to model the specimen in the nonpressurized condition, since the lateral stresses in this condition can reasonably be neglected. Because of lateral restraint provided by the applied pressure on the sides of the specimen, a plane strain solution was used to model the pressurized condition. Since the stress analyses were small-strain, linear elastic, and incompressible, the effect of the superimposed pressure on the propellant, liner, and insulation was to hydrostatically increase the stress state. Since this effect can be handled by simple superposition, the effect of superimposed pressure on *SR* is limited to the difference between the plane stress and plane strain solutions.

Since only stress ratios (not absolute stress values) were taken from the analytical stress distribution and used in the failure criteria evaluation calculations, time dependence was neglected. This method of data reduction is equivalent to assuming that the propellant, liner, and insulation follow a standard linear model of viscoelastic behavior. Experimentally, time dependence was taken into account by performing tests over a range of crosshead rates, running a log-log regression line through the values, and using the $t_m = 1$ min values for comparison.

Observations verifying the accuracy of the stress analyses include comparisons of analytically predicted and experimentally measured deformed geometries plus experimental failure-initiation locations that concur with analytical peak stress locations. Stress distribution plots, along with the additional details of the stress analyses, are given in Ref. 1.

Since only two-dimensional analyses were performed, it was necessary to assume that σ_3 was equal to the value of the superimposed pressure applied (e.g., $\sigma_3 = 0$ psig in the nonpressurized condition). This assumption is reasonably accurate since the major influences on the behavior of the specimen were in a plane.

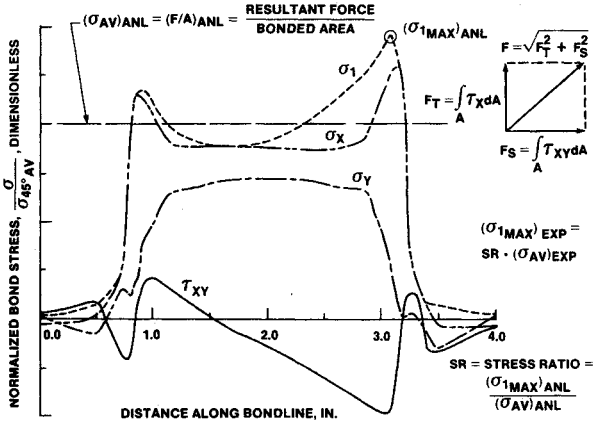

Fig. 3 Determination of the experimental value of peak stress at failure for the maximum principal stress at a 45 deg pull angle.

Table 1 Test data used in failure criterion investigation program

	Nonpressurized			Pressure = 1650 psig		
Pull angle, deg	Crosshead rate, in./min	Time to max stress, min	Maximum average stress, psi	Crosshead rate, in./min	Time to max stress, min	Maximum average stress, psi
	0.2	1.30	108	2	2.07×10^{-1}	287
	2.0	0.128	181	20	2.5×10^{-2}	474
90	2.0	0.162	159	200	2.0×10^{-3}	508
(Tension)	20.0	0.0172	273	1200	3.04×10^{-4}	706
	20.0	0.0157	203			
				200	1.9×10^{-3}	505
75	20.0	0.0155	225	1200	3.75×10^{-4}	679
	0.2	2.42	125	2	3.04×10^{-1}	244
	2.0	0.222	136	20	1.45×10^{-2}	215
60	2.0	0.264	148	20	3.70×10^{-2}	423
	20.0	0.025	205	200	3.2×10^{-3}	506
	20.0		215	1200	5.0×10^{-4}	600
	0.2	2.70	101	2	4.08×10^{-1}	209
	2.0	0.367	139	20	3.7×10^{-2}	284
45	2.0	0.288	139	200	3.7×10^{-3}	373
	20.0	0.030	158	1200	7.08×10^{-4}	479
	0.2	3.10	110	_[a]		
30	2.0	0.37	132	_[a]		
	20.0	0.0377	172	_[a]		
	0.2	4.38	109	_[a]		
15	2.0	0.426	127	_[a]		
	20.0	0.0391	166	_[a]		
	0.2	4.585	104	_[b]		
	0.2	4.70	120	_[b]		
0	2.0	0.533	131	_[b]		
(Shear)	2.0	0.0602	134	_[b]		
	20.0	0.0601	184	_[b]		

[a]Testing was performed but data was not usable due to specimen aging differences. [b]Not performed due to safety considerations.

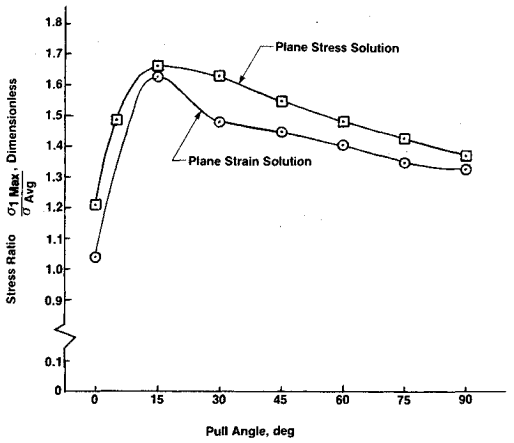

Fig. 4 Maximum principal to average stress ratio plotted vs pull angle.

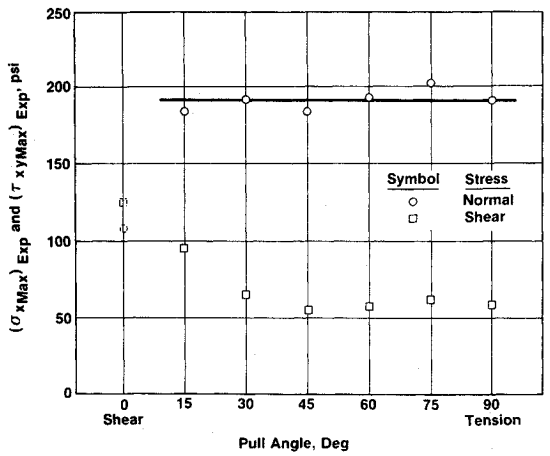

Fig. 5 Maximum bond normal and maximum bond shear stress at failure vs pull angle.

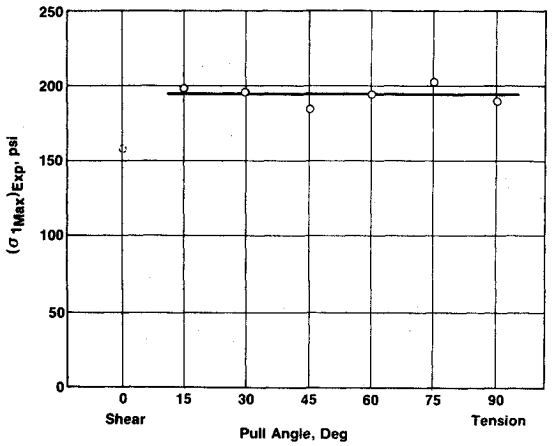

Fig. 6 Maximum principal stress at failure vs pull angle.

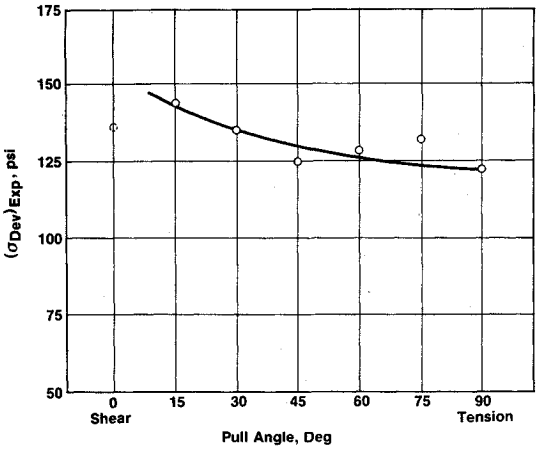

Fig. 7 Maximum deviatoric stress at failure vs pull angle.

Analytical/Experimental Correlation

To evaluate the failure criteria under consideration, it was necessary to relate the average stress-at-break value obtained from the experimental tests to the stress analysis of the specimen. The method is illustrated in Fig. 3 using σ_1 and a 45 deg pull angle as an example.

The first step in this process is to calculate the stress ratio *SR* for a given pull angle from the finite-element analysis. The two components necessary for calculating *SR* are 1) the average stress on the bondline, and 2) the maximum principal stress on the bondline. To calculate the average stress on the bondline, the total force F is determined by numerically integrating the finite-element stress distribution. Next, F is divided by the bonded area A to obtain the average stress value $(\sigma_{AVG})_{ANL}$. The maximum principal stress at the bondline, $(\sigma_{1\ MAX})_{ANL}$, is taken directly from the stress distribution. *SR* is then calculated by dividing $(\sigma_{1\ MAX})_{ANL}$ by $(\sigma_{AVG})_{ANL}$. The *SR* values calculated for the maximum principal stress failure criterion are plotted in Fig. 4.

Once *SR* is calculated, it can be multiplied by the average stress-at-failure value $(\sigma_{AVG})_{EXP}$ obtained from an actual bond test to yield the experimental value of the maximum principal stress at failure. Using this technique, it was possible to calculate the experimental values of the maximum bond normal and shear stress components, maximum principal stress, maximum deviatoric stress, and maximum shear stress as functions of the pull angle.

Experimental Error

It should be noted that the shear test data were obtained using "simple-shear" tests, where the end plates are allowed to move together during the test, as opposed to "true-shear" tests, where the end plates are held at a constant distance apart. The stress analysis data for the shear condition were obtained by modeling a "true-shear" test condition. Unpublished work by Bills showed that this difference in the shear test procedure can significantly influence the reported value of the bond shear strength.

Evaluation of the Failure Criteria

The failure criteria that provided nearly constant limiting values were the maximum bond normal and shear component stress criterion (Fig. 5), the modified maximum principal stress criterion (Fig. 6), the maximum deviatoric stress criterion (Fig. 7), and the maximum shear stress criterion (Fig. 8). An examination of the data shows that the maximum bond normal and maximum principal stress-at-failure values are both independent of the pull angle and differ only slightly in magnitude with the exception of the shear condition, while the maximum deviatoric and maximum shear stress-at-failure values appear to increase as they approach shear.

Since all failure criteria examined, except the modified maximum principal and the bond normal stress criteria, indicate changes in bond strength as the state of stress is varied, generalization to states of stress other than those of the test conditions would require testing at the pull angle reproducing the stress state of interest. The modified maximum principal and the maximum bond normal stress criteria can be general-

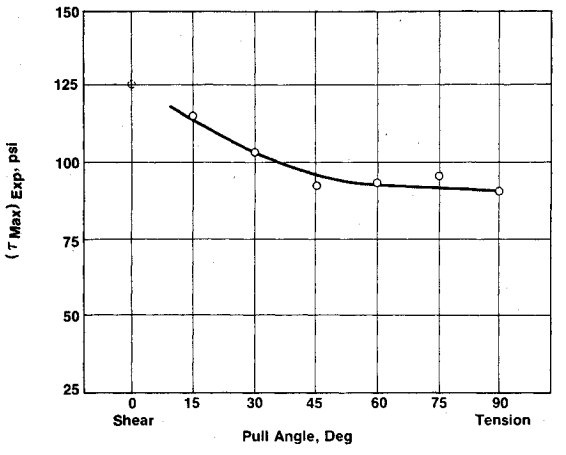

Fig. 8 Maximum shear stress at failure vs pull angle.

ized to other stress states based on a single test angle. Comparison of these two criteria show that the strength values are almost equal. A reasonable explanation for this agreement is the dominance of the tensile stress component at all test angles greater than 0 deg (see Ref. 1 for stress distribution plots). A possible explanation of why the maximum stress values obtained from the shear tests for these two criteria do not fall on the straight line formed by the data taken at the other pull angles is the lack of end tab restraint in the direction perpendicular to the load cell force in the shear test condition. If a "true-shear" test had been performed, the strength measurement would be higher and the data point would probably fall on the line. This fact must also be kept in mind when looking at the plots of the failure values for the other failure criteria. Experimental data from a "true-shear" test would provide valuable information as to which failure criterion is more accurate in this condition.

The data in Figs. 2 and 5-8 were taken at atmospheric pressure. Bond tests conducted at 1650 psig pressure using pull angles ranging from 45 to 90 deg produced similar bond strength trends (Fig. 2). A larger database would be helpful in refining the experimental differences among the failure criteria under consideration.

Further Investigation of the Modified Maximum Principal Stress Failure Criterion

An attempt was made to unify the pressurized and nonpressurized data by determining values for σ_{th} and a_p. Normally the threshold stress value σ_{th} would be obtained experimentally by performing constant-load tests and determining the stress value below which the bond system would not fail. This effort was not performed as part of the experimental test plan, so the σ_{th} value will only be used in relative terms in the data comparison. σ_{th} is related to the dewetting threshold, which varies somewhat with temperature and superimposed pressure.

The slopes of the log stress at failure vs log time-to-failure regression lines were obtained for both pressurized and nonpressurized conditions. It was found that the slope of the nonpressurized data was $m = -0.011$ and the pressurized data had a slope of $m = -0.013$. The difference in regression line slopes with a change in pressure is attributed to a difference in the threshold-stress values. In reducing the data, it was found that adding 61 psi to the stress-at-break values for the pressurized bond tests made the regression-line slopes of the pressurized condition the same as those of the nonpressurized condition. This is equivalent to saying that the difference in the σ_{th} values for the pressurized and nonpressurized conditions is about 61 psi.

Bills[6] found that the effect of superimposed pressure could be handled analytically through the use of a time pressure shift factor called a_p. After adding 61 psi to each of the stress-at-break values for the pressurized bond tests, a shift factor was calculated for each pull angle to make the regression line for the pressurized data fall on the regression line of the nonpressurized data. Applying a shift factor of 1050 (for 1650 psig) caused all the data points for a given pull angle to fall on approximately the same regression line (Fig. 9). The shift factor was experimentally determined to be the amount of shifting necessary to line up the regression lines of the pressurized and nonpressurized data. The value will be the same for all pull angles but different for each pressure. While the data used in this failure criteria investigation are limited, the modified maximum principal stress failure criterion appears to provide the best means of relating all parameters of the experimental test plan to a single failure quantity, i.e., $\sigma_1 - \sigma_{th}$.

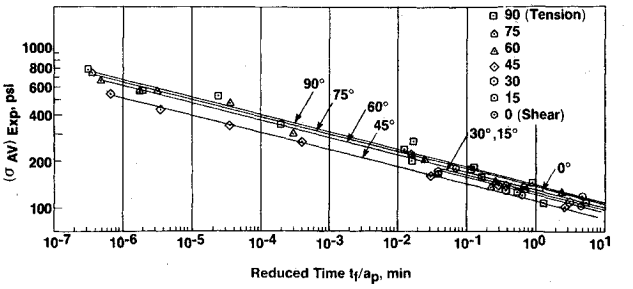

Fig. 9 Log stress vs log-reduced time regression lines through experimental test data (data adjusted for differences in threshold stress and superimposed pressure).

It is logical to calculate bondline margins of safety using a failure criterion based on the maximum principal stress because it represents the largest tensile stress at a point, regardless of orientation. In filled polymers that exhibit dewetting, such as solid propellants, the initial particle/polymer fractures cause high local deformations in the principal stress direction. These local elongations now concentrate the stresses such that failure is controlled by the largest of them. Even when these filled polymers carry shear loads, the high local deformations rearrange the geometry to carry the principal load as a tensile force. The chains "stretch" around the solid particles, elongating in the direction of the maximum principal stress. This behavior makes the stresses in any direction lateral to the principal stress direction much less significant.

Application

The modified maximum principal stress failure criterion is easy to implement. Analytically it requires using the quantity $\sigma_1 - \sigma_{th}$ as the "requirement" in the margin of safety calculation, where σ_1 is the peak principal stress value on the bondline of the motor (usually determined by finite-element analysis) and σ_{th} is determined experimentally. Determining the "allowable" requires (for a complete characterization) the determination of σ_{th} and a_p for each pressure and temperature, a_T for each temperature, and σ_0 and m. When testing is performed at the actual temperatures and pressures, it is not necessary to calculate each of these quantities because their only purpose is to relate the stress-at-break values obtained at particular test conditions to the values obtained under "standard" conditions. For tests at the actual conditions, the only modification to the average stress-at-break value is to multiply it by the appropriate stress ratio (obtained from stress analysis of the specimen) to provide the value of the maximum principal stress at failure and then subtract σ_{th}. This would be the "allowable" in the margin of safety calculation.

The modified maximum principal stress failure criterion has the advantage that specimens can be tested at any pull angle (excluding shear if "simple-shear" tests are used). This means that the data can be taken at the pull angle which produces the best specimen performance in terms of maintaining specimen

integrity, minimizing secondary bond failures, and avoiding undersirable failure types (e.g., hydrostatic tension). For the rectangular analog specimen, the optimum pull angle is 90 deg (tension). If desired, the specimen can be pulled at the angle which simulates the actual rocket motor bondline conditions to most closely simulate failure conditions.

Conclusion

Based on this preliminary evaluation, the following can be said for the modified maximum principal stress failure criterion: 1) it provides a determinable stress-at-break value for bond test specimens pulled over a range of pull angles, 2) it allows for changes in bond strength as a function of the time-to-failure, temperature, pressure, and state of stress, and 3) it is intuitively consistent with the type of failure that occurs in filled polymers. An improvement of the maximum bond normal and shear component failure criterion is realized by applying the appropriate stress concentration factors determined from the finite-element analyses of the bond specimen.

Further work should include expanding the database to include more temperatures and pressures, experimentally evaluating the effect of holding the endplates at a constant distance apart in the shear test, and experimentally evaluating σ_{th}. In addition, verification of the failure criterion in actual rocket or analog motors should be undertaken.

References

[1]Kuhlmann, T. L., Bills, K. W. Jr., and Peeters, R. L., "Propellant-Liner Bond Test Improvement Program," 1984 JANNAF CMCS/S&MBS Joint Subcommittee Meeting, CPIA Publication 418, Vol. 1, Chemical Propulsion Information Agency, Laurel, MD, Nov. 1984, p. 295.

[2]Anderson, J. M., Pavelka, T. D., and Bruno, P. S., "Techniques for Assessing Case Liner-Bond Integrity in Solid Propellant Rocket Motors," AFRPL-TR-73-75, Sept. 1973.

[3]Bills, K. W. Jr. and Schapery, R. A., "Liner Technology Program—Fracture Energy Method Development," AFRPL-TR-81-097, May 1982.

[4]Bills, K. W. Jr., "Investigation of Propellant-Liner Bonds and Development of Failue Criteria for Minuteman Wing II, Second Stage, Propellant-Liner Bond System," Aerojet Technical Memorandum 231, Aerojet-General Corp., Sacramento, CA, Aug. 1964.

[5]Becker, E. B. and Dunham, R. S., "Three-Dimensional Finite Element Computer Program Development—TEXGAP 2-D Documentation," AFRPL-TR-78-86, Feb. 1979.

[6]Bills, K. W. Jr., Sampson, R. C., Steele, R. D., Peterson, F. E., Briar, H. P., Plant, R. W. "Solid Propellant Cumulative Damage Program," AFRPL-TR-68-131, Oct. 1968.